Impaired fatty acid import or catabolism in macrophages restricts intracellular growth of *Mycobacterium tuberculosis*

Nelson V. Simwela[1], Eleni Jaecklein [2], Christopher M. Sassetti[2], David G. Russell[1]*

1. Department of Microbiology and Immunology, College of Veterinary Medicine, Cornell University, Ithaca, New York, USA
2. Department of Microbiology, UMass Chan Medical School, Worcester, Massachusetts, USA

*Correspondence: dgr8@cornell.edu

Abstract

Mycobacterium tuberculosis (*Mtb*) infection of macrophages reprograms cellular metabolism to promote lipid retention. While it is clearly known that intracellular *Mtb* utilize host derived fatty acids and cholesterol to fuel the majority of its metabolic demands, the role of macrophage lipid catabolism on the bacteria's ability to access the intracellular lipid pool remains undefined. We utilized a CRISPR genetic knockdown approach to assess the impact of sequential steps in fatty acid metabolism on the growth of intracellular *Mtb*. Our analyzes demonstrate that knockdown of lipid import, sequestration and metabolism genes collectively impair the intracellular growth of *Mtb* in macrophages. We further demonstrate that modulating fatty acid homeostasis in macrophages impairs *Mtb* replication through diverse pathways like enhancing production of pro-inflammatory cytokines, autophagy, restricting the bacteria access to nutrients and increasing oxidative stress. We also show that impaired macrophage lipid droplet biogenesis is restrictive to intracellular *Mtb* replication, but increased induction of the same by blockade of downstream fatty acid oxidation fails to rescue *Mtb* growth. Our work expands our understanding of how host fatty acid homeostasis impacts *Mtb* growth in the macrophage.

Significance

Mycobacterium tuberculosis (*Mtb*) primarily infects macrophages in the lungs. In infected macrophages, *Mtb* uses host lipids as key carbon sources to maintain infection and survive. In this work, we used a CRISPR-Cas9 gene knockout system in murine macrophages to examine the role of host fatty acid metabolism on the intracellular growth of *Mtb*. Our work shows that macrophages which cannot either import, store or catabolize fatty acids restrict *Mtb* growth by both common and divergent anti-microbial mechanisms, including increased glycolysis, increased production of reactive oxygen species, production of pro-inflammatory cytokines, enhanced autophagy and nutrient limitation. Our findings demonstrate that manipulating lipid metabolism in macrophages controls *Mtb* through multiple other mechanisms, beyond limiting the bacteria's access to nutrients.

Introduction

Mycobacterium tuberculosis (*Mtb*), the causative agent of tuberculosis (TB), has caused disease and death in humans for centuries (1). *Mtb* primarily infects macrophages in the lung (2, 3) wherein the bacterium relies on host derived fatty acids and cholesterol for synthesis of its lipid rich cell wall, and to produce energy and virulence factors (4-10). Within the lung microenvironment, resident alveolar macrophages preferentially oxidize fatty acids and are more permissive to *Mtb* growth while recruited interstitial macrophages are more glycolytic and restrictive of *Mtb* replication (11-13). Globally, *Mtb* infection modifies macrophage metabolism in a manner that enhances its survival. *Mtb* infected macrophages shift their mitochondrial substrate preference to exogenous fatty acids which drives the formation of foamy macrophages that are laden with cytosolic lipid droplets (4-6, 14, 15). Foamy macrophages are found in abundance in the central and inner layers of granulomas, a common histopathological feature of human TB (5, 16). Interference with key regulators of lipid homeostasis, such as the miR-33 and the transcription factors peroxisome proliferator-activated receptor α (PPARα) and PPAR-γ enhances macrophage control of *Mtb* (17-19). Moreover, compounds which modulate lipid metabolism such as the anti-diabetic drug metformin and some cholesterol lowering drugs are under investigation for host directed therapeutics (HDTs) against *Mtb* (20, 21). Although the dependence of intracellular *Mtb* on host fatty acids and cholesterol is well documented (22), the impact of specific aspects of macrophage lipid metabolism on the bacteria remains opaque. In *Mtb* infected foamy macrophages, bacteria containing phagosomes are found in close apposition to intracellular lipid droplets (4). It is believed that the bacterial induction of a foamy macrophage phenotype in host cells results in a steady supply of lipids that addresses the bacteria's nutritional requirements (4-7). In fact, intracellular *Mtb* has been shown to import fatty acids from host lipid droplet derived triacylglycerols (7). However, other studies indicate that macrophage lipid droplet formation in response to *Mtb* infection can lead to the induction of a protective, anti-microbial response (23). *Mtb* appears unable to acquire host lipids when lipid droplets are induced by stimulation with interferon gamma (IFN-γ) (23). Moreover, there is some evidence that lipid droplets can be sites for the production of host protective pro-inflammatory eicosanoids (7, 23). Lipid droplets can also act as innate immune hubs against intracellular bacterial pathogens by

clustering anti-bacterial proteins (24). Inhibition of macrophage fatty acid oxidation by knocking out mitochondrial carnitine palmitoyl transferase 2 (CPT2) or using chemical inhibitors of CPT2 also restrict intracellular growth of *Mtb* (11, 25). These data demonstrate that modulation of the different stages in lipid metabolism inside *Mtb* infected macrophages can result in conflicting outcomes.

We carried out a candidate-based, CRISPR mediated knockdown of lipid import and metabolism genes in macrophages to determine their roles in intracellular growth of *Mtb*. By targeting genes involved in fatty acid import, sequestration, and metabolism in Hoxb8 derived conditionally immortalized murine macrophages (26), we show that impairing lipid homeostasis in macrophages at different steps in the process negatively impacts the growth of intracellular *Mtb*, albeit to differing degrees. The impact on *Mtb* growth in the mutant macrophages was mediated through different mechanisms despite some common anti-microbial effectors. *Mtb* infected macrophages deficient in the import of long chain fatty acids increased production of pro-inflammatory markers such as interleukin 1β (IL-1β). In contrast, ablation of lipid droplet biogenesis and fatty acid oxidation increased production of reactive oxygen species and limited the bacteria's access to nutrients. We also found that suppression of *Mtb* growth in macrophages that are unable to produce lipid droplets could not be rescued by exogeneous addition of fatty acids indicating that this is not purely nutritional restriction. Our data indicate that interference of lipid metabolism in macrophages leads to suppression of *Mtb* growth via multiple routes.

Results

Knockdown of fatty acid import and metabolism genes restricts *Mtb* growth in macrophages

To apply a holistic approach to assessing the role(s) of fatty acid metabolism on the intracellular growth of *Mtb*, we used a CRISPR genetic approach to knockout genes involved in lipid import (CD36, FATP1), lipid droplet formation (PLIN2) and fatty acid oxidation (CPT1A, CPT2) in mouse primary macrophages (Fig. 1A). Deletion of CD36 or CPT2 from mouse macrophages has been shown to impair intracellular growth of *Mtb* (25, 27). But the role of specialized long chain fatty acid transporters (FATP1-6) on *Mtb* growth in macrophages is uncharacterized. FATP1 and FATP4 are the most abundant fatty acid transporter isoforms in macrophages (28). PLIN2, or adipophilin, is known to be required for lipid droplet formation (29, 30). Five isoforms of mammalian perilipins (PLIN) are involved in lipid droplet biogenesis amongst which PLIN2 is the dominant isoform expressed in macrophages (23). However, macrophages derived from PLIN2$^{-/-}$ mice show no defects in production of lipid droplets nor do they impair intracellular growth of *Mtb* (23). We targeted each of these genes with at least 2 sgRNAs in Hoxb8 Cas9^{+} conditionally immortalized myeloid progenitors (26) to generate a panel of mutants that were deficient in the following candidates of interest; FATP1$^{-/-}$, PLIN2$^{-/-}$, CD36$^{-/-}$, CPT1A$^{-/-}$ and CPT2$^{-/-}$. Each individual sgRNA achieved >85% CRISPR-mediated deletion efficiency for all the 5 genes, as analyzed by the Inference for CRISPR Edits (ICE) tool (31) (Table. S1). We verified the protein knockdown phenotypes by flow cytometry and western blot analysis of differentiated macrophages derived from the CRISPR deleted Hoxb8 myeloid precursors (Fig. S1).

To confirm certain knockdown phenotypes functionally, we checked lipid droplet biogenesis in PLIN2$^{-/-}$ macrophages in comparison to macrophages transduced with a non-targeting scramble sgRNA by confocal microscopy of BODIPY stained cells. Cells were cultured for 24 hours in the presence of exogenous oleate to enhance the formation of lipid droplets (32). We observed a complete absence of lipid droplet formation in PLIN2$^{-/-}$ macrophages as compared to controls (Fig. S2). This is contrary to previous observations in macrophages derived from PLIN2 knockout mice which were reported to have no defect in lipid droplet formation (23). We also assessed the ability of CPT2$^{-/-}$ macrophages to oxidize fatty acids using the Agilent Seahorse XF Palmitate Oxidation Stress Test. Scrambled sgRNA and CPT2$^{-/-}$ macrophages were cultured in

substrate limiting conditions and supplied with either bovine serum albumin (BSA) or BSA conjugated palmitate. As shown in Fig. S2B, control macrophages were able to utilize and oxidize palmitate in substrate limiting conditions indicated by a significant increase in oxygen consumption rates (OCRs) in contrast to cells supplied with BSA alone. Addition of the CPT1A inhibitor, etomoxir, inhibited the cell's ability to use palmitate in these conditions (Fig. S2B). CPT2 knockdown in CPT2$^{-/-}$ macrophages impaired the cell's ability to oxidize palmitate to a degree comparable to etomoxir treatment as evidenced by baseline OCRs when compared to scrambled sgRNA control (Fig. S2C).

We then assessed the different knockdown mutant macrophages in their ability to support the intracellular growth of *Mtb*. We infected macrophages with *Mtb* Erdman at a multiplicity of infection (MOI) of 0.4 and assessed intracellular bacterial growth rates by counting colony forming units (CFUs) 5 days post infection. All the 5 mutant macrophages significantly impaired *Mtb* growth rates when compared to scrambled sgRNA as assessed by CFUs counts on day 5 (Fig. 1C). PLIN2$^{-/-}$, FATP1$^{-/-}$ and CPT2$^{-/-}$ macrophages displayed the strongest growth restriction phenotypes while CD36$^{-/-}$macrophages had a moderate, but significant, impact on *Mtb* growth. We quantified intracellular bacteria on day 0, 3 hours post infection (Fig. 1B), to ascertain that subsequent differences on day 5 were not due to defects in initial phagocytosis. The moderate growth restriction phenotypes of CD36$^{-/-}$ macrophages were consistent with previous findings which reported similar impact on *Mtb* and *M. marinum* growth in macrophages derived from CD36$^{-/-}$ mice (27). Impaired growth of *Mtb* in CPT1A$^{-/-}$ and CPT2$^{-/-}$ macrophages is also consistent with previous reports that genetic and chemical inhibition of fatty acid oxidation is detrimental to the growth of *Mtb* within macrophages (11, 25).

Mtb infected macrophages with impaired fatty acid import and metabolism display altered mitochondrial metabolism and elevated glycolysis.

Impairment of fatty acids metabolism by FATP1 knockout in macrophages rewires their substrate bias from fatty acids to glucose (33). We reasoned that deletion of genes required for downstream processing of lipids (Fig. 1A) could also reprogram macrophages and increase glycolysis which could, in part, explain bacterial growth restriction. We analyzed the metabolic states of 3

knockout macrophages (FATP1$^{-/-}$, PLIN2$^{-/-}$ and CPT2$^{-/-}$) in uninfected and *Mtb* infected conditions by monitoring oxygen consumption rates (OCR) and extracellular acidification rates (ECARs) using the Agilent Mito and Glucose Stress Test kits. All 3 mutant uninfected macrophages displayed reduced mitochondrial respiration as evidenced by lower basal and spare respiratory capacity (SRC) when compared to scrambled sgRNA controls (Fig. S3A, 3SB). *Mtb* infection proportionally reduced basal and SRC rates across all the mutant macrophages and scrambled controls (Fig. 2A, 2B) when compared to uninfected macrophages, which is consistent with previous findings (14). PLIN2$^{-/-}$ macrophages displayed the most marked reduction in mitochondrial activity in both uninfected and infected conditions, while FATP1$^{-/-}$ macrophages were the least affected (Fig. 2A, Fig. S3A). As reported previously (33), uninfected FATP1$^{-/-}$ macrophages were more glycolytically active with higher basal and spare glycolytic capacity (SGC) compared to scrambled controls (Fig. S3D, S3E). Uninfected PLIN2$^{-/-}$ and CPT2$^{-/-}$ macrophages were also more glycolytically active, but to a greater degree than FATP1$^{-/-}$ (Fig. S3D, S3E). *Mtb* infection increased the glycolytic capacity of all the 3 mutant macrophages (Fig. 2C, 2D). Overall, PLIN2$^{-/-}$ macrophages exhibited the highest glycolytic capacity (Fig. 2C, Fig. S3D). Our data indicates that impairment of fatty acid metabolism at different steps significantly impacts mitochondrial respiration and reprograms cells towards glycolysis. Increased glycolytic flux in macrophages has been linked to the control of intracellular *Mtb* growth (34, 35). Metabolic realignment as a consequence of interference with lipid homeostasis, which results in enhanced glycolysis may contribute to *Mtb* growth restriction in these mutant macrophages.

Knockdown of lipid import and metabolism genes in macrophages activates AMPK and stabilizes HIF-1α

Mtb infection is known to induce increased glycolysis or the “Warburg effect” in macrophages, mouse lungs and human TB granulomas (34-36). Several studies have demonstrated that the Warburg effect is mediated by the master transcription factor hypoxia-inducible factor-1 (HIF-1) (37). During *Mtb* infection, HIF-1 is activated by production of reactive oxygen species (ROS), TCA cycle intermediates and hypoxia in the cellular microenvironments as a consequence of altered metabolic activities and increased immune cell functions (34-36, 38). We assessed HIF-1 stability

in the 3 mutant macrophage lineages (FATP1$^{-/-}$, PLIN2$^{-/-}$ and CPT2$^{-/-}$) by monitoring total HIF-1α protein levels by western blot, having confirmed that they were all more glycolytically active than the scrambled controls (Fig. 2, Fig. S3). Indeed, all the 3 mutant macrophages displayed significantly higher amounts of total HIF-1α when compared to scrambled controls in uninfected conditions and after *Mtb* infection for 48 hours (Fig. 3A, 3B). We also checked the phosphorylation status of the adenosine monophosphate kinase (AMPK), a master regulator of cell energy homeostasis (39), in the mutant macrophages since Seahorse flux analyses indicated that they had impaired mitochondrial activities (Fig. 2, Fig. S3). Western blot analysis revealed that in both *Mtb* infected and uninfected conditions, impaired fatty acid metabolism correlated with moderate activation of AMPK as indicated by increased AMPK phosphorylation (Fig. 3C, 3D). These data point to a metabolic reprogramming of cells through activation of HIF-1α and AMPK to promote glycolysis. In energetically stressed cellular environments, activated AMPK promotes catabolic processes such as autophagy to maintain nutrient supply and energy homeostasis (39). Autophagy is also an innate immune defense mechanism against intracellular *Mtb* in macrophages (40). We examined the levels of autophagic flux in the mutant macrophages by monitoring LC3I to LC3II conversion by western blot and by qPCR analysis of selected autophagy genes (*AMBRA1*, *ATG7*, *MAP1LC3B* and *ULK1)*. We observed a moderate increase in autophagic flux by western blot in uninfected FATP1$^{-/-}$ and CPT2$^{-/-}$ macrophages, which was amplified upon infection with *Mtb* (Fig. S4A, S4B). Our qPCR analysis revealed that the 4 autophagy genes were upregulated in both *Mtb* infected and uninfected conditions in all the 3 mutants (Fig. S4C, S4D). These data suggest that impaired fatty acid import and metabolism in macrophages could be restricting *Mtb* growth by promoting autophagy. These data agree with previous observations that inhibition of fatty acid oxidation enhances macrophage xenophagic activity whichleads to improved control of *Mtb* (25).

Exogenous oleate fails to rescue the *Mtb icl1*-deficient mutant in FATP1$^{-/-}$, PLIN2$^{-/-}$ and CPT2$^{-/-}$ macrophages

The mycobacterial isocitrate lyase (*icl1*) acts as an isocitrate lyase in the glyoxylate shunt and as a methyl-isocitrate lyase in the methyl-citrate cycle (MCC) (41, 42). *Mtb* uses the MCC to convert

propionyl CoA originating from the breakdown of cholesterol rings and β-oxidation of odd chain fatty acids into succinate and pyruvate, which are eventually assimilated into the TCA cycle (43, 44). The buildup of propionyl CoA is toxic to *Mtb* and the bacteria relies on the MCC together with the incorporation of propionyl CoA to methyl-branched lipids in the cell wall as an internal detoxification system (43, 45). *Mtb* propionyl CoA toxicity is, in part, due to a cellular imbalance between propionyl CoA and acetyl CoA as an accumulation of the former or paucity of the latter results in the propionyl CoA mediated inhibition of pyruvate dehydrogenase (46). Consequently, *Mtb icl1* deficient mutants (*Mtb ⊿icl1*) are unable to grow in media supplemented with cholesterol or propionate, or intracellularly in macrophages (46). However, this growth inhibition could be rescued both in culture and in macrophages by exogenous supply of acetate or even chain fatty acids which can be oxidized to acetyl-CoA (46). We took advantage of this metabolic knowledge to assess whether exogenous addition of the even chain fatty acid oleate can rescue the intracellular growth of *Mtb ⊿icl1* mutants in our CRISPR knockdown macrophages. Scrambled controls, FATP1$^{-/-}$, PLIN2$^{-/-}$ and CPT2$^{-/-}$ macrophages in normal macrophage media or media supplemented with oleate were infected with an *Mtb ⊿icl1* strain expressing mCherry at MOI 5. Bacterial growth measured by mCherry expression was recorded 5 days post infection. Consistent with previous observations (46), the *Mtb ⊿icl1* mutant failed to replicate in both mutant and scramble macrophages that were grown in normal macrophage media as evidenced by baseline mCherry fluorescence (Fig. 4A). Oleate supplementation successfully rescued the *Mtb ⊿icl1* mutant in scrambled control macrophages. However, the growth restriction of the *Mtb ⊿icl1* strain could not be alleviated by exogenous addition of oleate to the mutant macrophages (FATP1$^{-/-}$, PLIN2$^{-/-}$ and CPT2$^{-/-}$) (Fig. 4A). These data suggest that impaired import (FATP1$^{-/-}$), sequestration (PLIN2$^{-/-}$) or β-oxidation of fatty acids (CPT2$^{-/-}$) blocks *Mtb*'s ability to access and use cellular lipids.

Oleate supplementation in macrophages induces the formation of lipid droplets and we were able to confirm the inability to produce lipid droplets in PLIN2$^{-/-}$ macrophages using this approach (Fig. S2A). As an indirect measure to track the fate of supplemented oleate in the mutant macrophages, we monitored lipid droplet biogenesis in FATP1$^{-/-}$ and CPT2$^{-/-}$ macrophages to check if the inability to rescue the *Mtb ⊿icl1* impaired growth phenotypes in these mutant macrophages could be possibly related to disruptions in lipid droplet biogenesis. Confocal analysis

of BODIPY stained cells upon oleate supplementation revealed that FATP1$^{-/-}$ macrophages also fail to generate lipid droplets (Fig. 4B). In contrast, CPT2$^{-/-}$ macrophages produced more and larger lipid droplets in comparison to scrambled controls (Fig.4B). These data suggest that the inhibition of *Mtb* growth in these mutant macrophages is not merely through limitation of access to fatty acid nutrients.

Dual RNA sequencing to identify host and bacterial determinants of *Mtb* restriction in mutant macrophage lineages.

We performed RNA sequencing of both host and bacteria in *Mtb* infected mutant macrophages as a preliminary step in identification of pathways restricting bacterial growth. We infected scrambled controls, FATP1$^{-/-}$, PLIN2$^{-/-}$ and CPT2$^{-/-}$ macrophages with the *Mtb* smyc'::mCherry strain for 4 days and processed the samples for dual RNA sequencing as previously described (47). Principal component analysis (PCA) of host transcriptomes revealed a clustering of all the 3 mutant macrophages away from scrambled controls (Fig. 5A). Interestingly, there was a separation in transcriptional responses between the 3 mutant macrophages as CPT2$^{-/-}$ and PLIN2$^{-/-}$ macrophages clustered closer together and more distant from FATP1$^{-/-}$ (Fig. 5A). Overall, using an adjusted p-value < 0.05 and absolute log2 fold change > 1.2, we identified 900 genes which were differentially expressed (DE) in PLIN2$^{-/-}$ macrophages (589 up, 311 down), 817 genes which were DE in FATP1$^{-/-}$ macrophages (501 up, 315 down) and 189 genes which were DE in CPT2$^{-/-}$ (124 up, 65 down) (Table. S2, Fig.5B). Consistent with the PCA analysis, Venn diagram of the DE genes (Fig.5B) indicated divergent responses in the 3 mutant macrophage populations. We performed pathway enrichment analysis (48) of the DE genes to identify anti-microbial pathway candidates in the 3 mutant macrophages. We found that defects in fatty acid uptake in FATP1$^{-/-}$ infected macrophages upregulated pro-inflammatory pathways involved in MAPK and ERK signaling and production of inflammatory cytokines (IFN-γ, interleukin-6, Interleukin-1α, β) (Fig. 5D, Table. S3). The pro-inflammatory signatures of the FATP1$^{-/-}$ macrophages are consistent with previous observations that demonstrated that a deficiency in FATP1 exacerbated macrophage activation *in vitro* and *in vivo* (33). FATP1 is a solute carrier family member (SLC27A1) and *Mtb* infected FATP1$^{-/-}$ macrophages showed reduced expression of other solute carrier transporters

(SLC) such as FATP4 (SLC27A4), GLUT1 (SLC2A1) and 8 SLC amino acid transporters (Fig. S7A, S7B, Table. S2). Interestingly, *Mtb* infected FATP1$^{-/-}$ macrophage transcriptomes exhibited upregulation of macrophage scavenger receptors (MSR1) and the ATP binding cassette transporter ABCC1 (Fig. S7A), both of which can independently transport fatty acids into cells (49, 50).

Meanwhile, inability generate lipid droplets in *Mtb* infected PLIN2$^{-/-}$ macrophages led to upregulation in pathways involved in ribosomal biology, MHC class 1 antigen presentation, canonical glycolysis, ATP metabolic processes and type 1 interferon responses (Fig. 5C, Table. S3). In the downregulated PLIN2$^{-/-}$ DE gene set, enriched pathways included those involved in production of pro-inflammatory cytokines; interleukin-6 and 8, IFN-γ and interleukin-1 (Fig. S5A, Table. S3). Oxidative phosphorylation and processes involved in the respiratory chain electron transport were also significantly enriched in PLIN2$^{-/-}$ downregulated genes. This suggests that *Mtb* infected PLIN2$^{-/-}$ macrophages increase glycolytic flux and decrease mitochondrial activities, which is consistent with our metabolic flux analysis data (Fig.2). Unlike FATP1$^{-/-}$ macrophages, PLIN2$^{-/-}$ macrophages are, however, broadly anti-inflammatory as most pro-inflammatory genes were downregulated upon *Mtb* infection.

Further downstream in the lipid processing steps, inhibition of fatty acid oxidation in CPT2$^{-/-}$ macrophages upregulated pathways involved in MHC class 1 antigen presentation, response to IFN-γ and interleukin-1 and T-cell mediated immunity (Fig. S6, Table. S3). There was a limited overlap in enriched pathways in the upregulated genes between *Mtb* infected CPT2$^{-/-}$ and FATP1$^{-/-}$ macrophages such as those involved in the cellular responses to interleukin-1 and IFN-γ. However, many pathways over-represented in CPT2$^{-/-}$ macrophages were common to PLIN2$^{-/-}$ macrophages (Fig. 5C, Fig. S6, Table. S3). Similarly, both *Mtb*-infected PLIN2$^{-/-}$ *and* CPT2$^{-/-}$ macrophages were downregulated in expression of genes involved in oxidative phosphorylation (Table. S3). We confirmed expression levels of key genes by qPCR analysis of IL-1β and the type 1 interferon (IFN-β) response during the early time points of infection. Indeed, 4 hours post infection, IL-1β and IFN-β were both upregulated in FATP1$^{-/-}$ macrophages as compared to scrambled controls consistent with their pro-inflammatory phenotype (Fig. S8A, S8B). On the contrary, PLIN2$^{-/-}$ macrophages downregulated IL-1β (Fig. S8B). These data indicate that

macrophages respond quite divergently to the deletion of the different steps in fatty acid uptake, which implies that the intracellular pressures to which *Mtb* is exposed may also differ.

Oxidative stress and nutrient limitation are major stresses experienced by *Mtb* in PLIN2$^{-/-}$ and CPT2$^{-/-}$ macrophages

We also analyzed transcriptomes from intracellular *Mtb* from scrambled controls, FATP1$^{-/-}$, CPT2$^{-/-}$ and PLIN2$^{-/-}$ macrophages in parallel with host transcriptomes in Fig. 5A. Using an adjusted p-value of < 0.1 and an absolute log2 fold change > 1.4, 0 genes were DE in FATP1$^{-/-}$ macrophages, 105 *Mtb* genes were DE in PLIN2$^{-/-}$ macrophages (69 up, 36 down) and 10 genes were DE in CPT2$^{-/-}$ macrophages (3 up, 7 down) (Fig. 6A). Despite being restrictive to *Mtb* growth (Fig. 1C) and appearing more pro-inflammatory (Fig. 5D), FATP1$^{-/-}$ macrophages did not elicit a detectable shift in the transcriptional response in *Mtb,* compared to control host cells. We speculate that pro-inflammatory responses in FATP1$^{-/-}$ macrophages could be enough to restrict the growth of bacteria, but the resulting compensatory responses as evidenced by the upregulation of macrophage scavenger receptors (Fig. S7A) alleviate some of the stresses that a lack of fatty acid import could be duly exerting on the bacteria. PLIN2$^{-/-}$ macrophages appeared to elicit the strongest transcriptional response from *Mtb* which is consistent with our CFU data (Fig. 1C) as PLIN2$^{-/-}$ macrophages exhibited the strongest growth restriction. Among the DE genes in *Mtb* from PLIN2$^{-/-}$ macrophages, a significant number of upregulated genes are involved in nutrient assimilation (Fig. 6B). *Mtb* in PLIN2$^{-/-}$ macrophages upregulated CobU (Rv0254c) which is predicted to be involved in the bacteria's cobalamin (Vitamin B_{12}) biosynthesis. Vitamin B_{12} is an important cofactor for the activity of *Mtb* genes required for cholesterol and fatty acid utilization (45, 51). Genes involved in de novo long chain fatty acid synthesis (AccE5, Rv281) (52), cholesterol breakdown (HsaD, Rv3569c) (53), β-oxidation of fatty acids (EchA18, Rv3373; FadE22, Rv3061c) (54), purine salvage (Apt, Rv2584c) (55) and tryptophan metabolism (56) were also upregulated in *Mtb* from PLIN2$^{-/-}$ macrophages (Fig. 6B). This metabolic re-alignment response is seen most frequently under nutrient limiting conditions (11, 12, 57). *Mtb* in PLIN2$^{-/-}$ macrophages also appears to experience a significant level of other cellular stresses as genes involved in DNA synthesis and repair, general response to oxidative stress and PH survival in the phagosome

(DnaN, Rv0002; RecF, Rv0003; DinF, Rv2836c; Rv3242c, Rv1264) were upregulated (Fig. 6B). Amongst the down-regulated genes in *Mtb* in PLIN2$^{-/-}$ macrophages, FurA (Rv1909c), a KatG repressor was the most significant (Fig. 6B, Table. S4). FurA downregulation derepresses the catalase peroxidase, KatG, which promotes *Mtb* survival in oxidative stress conditions (58). These data suggest that PLIN2$^{-/-}$ macrophages could be, in part, restricting *Mtb* growth by increasing production of ROS. The data also suggest that, contrary to a previous report (23), blocking lipid droplet formation in host macrophages does place increased nutritional and oxidative stress on intracellular *Mtb*.

CPT2$^{-/-}$ macrophages elicited a modest shift in transcriptional response from *Mtb*, and the majority of the DE genes (8 out of 10) were also DE in PLIN2$^{-/-}$ macrophages (Table. S4). This in in agreement with the host transcription response as CPT2$^{-/-}$ and PLIN2$^{-/-}$ macrophages share similar candidate anti-bacterial responses (Fig.5A-C, S5). In common with the *Mtb* transcriptome response in PLIN2$^{-/-}$ macrophages, upregulated genes in *Mtb* isolated from CPT2$^{-/-}$ macrophages included those involved in response to oxidative stress (DinF, Rv2836c) (Table. S4). To substantiate some of these pathways, we assessed the levels of total cellular ROS in FATP1$^{-/-}$, PLIN2$^{-/-}$ and CPT2$^{-/-}$ macrophages in both *Mtb* infected and uninfected conditions by staining the cells with the Invitrogen CellROX dye and confocal microscopy analysis of live stained cells. In both infected and uninfected conditions, all the 3 mutants displayed significantly elevated total cellular ROS when compared to scramble controls (Fig. S9A, S9B).

Inhibitors of lipid metabolism block intracellular growth of *Mtb* in macrophages but not in broth culture

We next examined if pharmacological inhibitors would phenocopy the growth inhibition phenotypes we observed with specific gene deletions. Compounds which modulate lipid homeostasis are currently being investigated for HDT against TB, which is an area of considerable interest (59). Such compounds include metformin, a widely used anti-diabetic drug which activates AMPK, inhibits fatty acid synthesis and promotes β-oxidation of fatty acids (21, 60). Chemical inhibition of fatty acid β-oxidation is already known to promote macrophage control of *Mtb* (11, 25). We targeted macrophage lipid homeostasis with trimetazidine (TMZ), an inhibitor

406 of β-oxidation of fatty acids, metformin, and an FATP1 inhibitor, FATP1 In (61). We assessed the
407 impact of these compounds on extracellular *Mtb* cultured in broth over 9 days in the presence of
408 the inhibitors (DMSO, TMZ; 500 nM, Metformin; 2 mM, FATP1 In; 10 μM, Rifampicin; 0.5 μg/ml).
409 None of the 3 lipid metabolism inhibitors had a measurable effect on *Mtb* growth in liquid culture
410 media when compared to DMSO controls (Fig. 7A). Treatment with rifampicin completely blocked
411 bacterial growth under the same conditions (Fig. 7A). We next infected scrambled sgRNA control
412 macrophages with *Mtb* at MOI 0.5. Inhibitors were added to infected macrophages 3 hours post
413 infection and bacterial CFUs were enumerated 4 days post treatment. Consistent with previous
414 observations (21, 25), TMZ and metformin significantly reduced bacterial loads in macrophages
415 when compared to DMSO controls (Fig.7B). Similarly, FATP1 In also impacted the intracellular
416 growth of *Mtb* (Fig. 7B). The results provide independent data that both genetic and chemical
417 modulation of fatty acid metabolism at different steps in the process negatively impacts
418 intracellular growth of *Mtb*.
419
420 **Discussion**
421 It is clearly established that host derived fatty acids and cholesterol are important carbon sources
422 for *Mtb* (22). However, the relationship between *Mtb* and the infected host cell lipid metabolism
423 remains a subject of conjecture. In this report, we characterized the role of macrophage lipid
424 metabolism on the intracellular growth of *Mtb* by a targeted CRISPR mediated knockout of host
425 genes involved in fatty acid import, sequestration and catabolism. Macrophage fatty acid uptake
426 is mediated by the scavenger receptor CD36 and specialized long chain fatty acid transporters,
427 FATP1 and FATP4 (62). Earlier studies reported that a deficiency of CD36 enhances macrophage
428 control of *Mtb,* albeit to a modest degree (27). Work from Hawkes et al.(27) indicated that the
429 anti-microbial effectors in CD36 deficient macrophages were not due to bacterial uptake
430 deficiencies, differences in the rate of *Mtb* induced host cell death, production of ROS or pro-
431 inflammatory cytokines (27). We similarly observed a moderate *Mtb* growth restriction
432 phenotype in our CRISPR generated $CD36^{-/-}$ macrophages. However, a strong growth restriction
433 of *Mtb* was observed when we knocked out the long chain fatty acid transporter, FATP1. $FATP1^{-/-}$
434 macrophages displayed altered metabolism characterized by stabilization of HIF-1α, activated

AMPK, increased glycolysis and reduced mitochondrial functions. Given that both CD36 and FATP1 perform similar functions, it is expected that they should be some degree of compensation between the transporters when either of the genes are deleted. Indeed, we found out that FATP1 knockout resulted in the upregulation of other lipid import transporters (MSR1, ABCC1). This would be consistent with the moderate anti-*Mtb* phenotypes in CD36$^{-/-}$ macrophages which could easily be compensated by the presence of FATPs to alleviate the reduction in fatty acid supply experienced by intracellular *Mtb*. However, the FATP1$^{-/-}$ macrophage phenotype appears to be more severe on *Mtb* and could be exacerbated by an elevated pro-inflammatory response as has been reported previously both *in vitro* and *in vivo* (33).

After uptake into the cells, most fatty acids either undergo β-oxidation in the mitochondria to provide energy or are esterified with glycerol phosphate to form triacylglycerols that may be incorporated into lipid droplets in the endoplasmic reticulum (62). Over the last 2 decades, it has been believed that lipid droplets are a nutrient source for *Mtb* in macrophages (4-7). However, recent work indicates lipid droplets may serve as centers for the production of pro-inflammatory markers and anti-microbial peptides (23, 24). It has also been reported that bone marrow macrophages derived from PLIN2$^{-/-}$ mice did not have defects in the formation of lipid droplets and supported robust intracellular *Mtb* replication (23). However, our mutant macrophages with myeloid specific knockout of PLIN2 are unable to form lipid droplets and are defective in supporting the growth of *Mtb*. The discrepancies with previous observations (23) could be a consequence of compensatory responses to PLIN2 knockout in whole mice which when performed at embryonic level would allow for sufficient time for the cells to recover by upregulating related PLIN isoforms. In fact, PLIN2$^{-/-}$ macrophages displayed the strongest anti-*Mtb* phenotypes amongst our mutants exhibiting activated AMPK, increased glycolysis and autophagy and impaired mitochondrial functions. *Mtb* isolated from PLIN2$^{-/-}$ macrophages displayed signatures of severe nutrient limitation and oxidative stress damage.

It has also been previously reported that chemical, genetic or miR33 mediated blockade of fatty acid β-oxidation in macrophages induces lipid droplet formation (19, 25) but that this enhanced lipid droplet formation does not correlate with improved intracellular *Mtb* growth (25).

We observed a similar phenotype as CPT2$^{-/-}$ macrophages that generated larger and more abundant lipid droplets than scrambled control macrophages were still restrictive to *Mtb* growth. This implies that the presence or absence of lipid droplets does not in itself indicate whether a macrophage will support or restrict *Mtb* growth, and that the anti-microbial environment extends beyond simple nutrient availability.

In summary, our study shows that blocking macrophage's ability to import, sequester or catabolize fatty acids chemically or by genetic knockdown impairs *Mtb* intracellular growth. There are shared features between potential anti-microbial effectors in macrophages which lack the ability to import (FATP$^{-/-}$) or metabolize fatty acids (PLIN2$^{-/-}$, CPT2$^{-/-}$) such as increased glycolysis, stabilized HIF-1α, activated AMPK, enhanced autophagy and production of ROS. However, there are also intriguing points of divergence as FATP$^{-/-}$ macrophages are more pro-inflammatory while PLIN2$^{-/-}$ macrophages appear to be broadly anti-inflammatory. The routes to *Mtb* growth restriction in these mutant macrophages are clearly more complex than the bacteria's inability to acquire nutrients. The data further emphasizes that targeting fatty acid homeostasis in macrophages at different steps in the process (uptake, storage and catabolism) is worthy of exploring in the development of new therapeutics against tuberculosis.

Materials and methods

All materials and methods are as described (47) unless otherwise specified.

Flow cytometry and western blot analysis

Generation of CRISPR mutant Hoxb8 macrophages was carried out described previously (47). Antibodies used for both western blot and flow cytometry were as follows: rat anti-Mouse CD36:Alexa Fluor®647 (Biorad, 10 µl/million cells), rabbit anti-PLIN2 (Proteintech, 1:1000), rabbit anti-FATP1 (Affinity biosciences, 1:1000), rabbit anti-CPT1A antibody (Proteintech, 1:1000), rabbit anti-CPT2 antibody (Proteintech, 1:1000), rabbit anti-HIF-1α antibody (Proteintech, 1:1000), rabbit anti-AMPKα(1:1000, Cell signalling Technology), rabbit anti-Phospho-AMPKα(1:500, Cell signalling Technology), rabbit anti-LC3B (1:1000, Cell signalling Technology) and rabbit anti-β Actin (1:1000, Cell Signalling Technology). For western blots, secondary antibodies used were anti-rabbit/mouse StarBright Blue 700 (1:2500, Biorad). Blots were developed and imaged as described previously (47).

Staining for cellular lipid droplets

Macrophages monolayers in Ibidi eight-well chambers were supplemented with exogenous 400 µM oleate for 24 hours to induce the formation of lipid droplets (32). Cells were then fixed in 4% paraformaldehyde and stained with BODIPY™ 493/503 (Invitrogen, 1 µg/ml) in 150 mM sodium chloride. Stained cells were mounted with media containing DAPI and imaged using a Leica SP5 confocal microscope.

Seahorse XF palmitate oxidation stress test

A modified Seahorse mitochondrial stress test was used to measure macrophage's ability to oxidize palmitate in substrate limiting conditions. 2 days before the assay, 1 x 10^5 cells were plated in Seahorse cell culture mini plates. 1 day before the assay, macrophage media was replaced with the Seahorse substrate limited growth media (DMEM without pyruvate supplemented with 0.5 mM glucose, 1 mM glutamine, 1% FBS and 0.5 mM L-Carnitine). On the day of the assay, substrate limited media was replaced with assay media (DMEM without pyruvate supplemented with 2 mM

glucose and 0.5 mM L-Carnitine). In selected treatment conditions, cells were either supplied with bovine serum albumin (BSA), BSA palmitate or BSA palmitate plus etomoxir (4 µM). Oxygen consumption rates (OCRs) were measured using the Mito Stress Test assay conditions as described previously (47).

Rescue of the *Mtb* Δicl1 mutant in oleate supplemented media

The *Mtb* H37Rv Δ*icl1* mutant expressing mCherry (46) was used for the rescue experiments. The strain was maintained in 7H9 OADC broth as previously described (47) in the presence of Kanamycin (25 µg/ml) and hygromycin (50 µg/ml). 24 hours before infection, macrophages were cultured in normal macrophage media or media supplemented with 400 µM oleate. Cells were then infected with the *Mtb* Δ*icl1* mutant at MOI 5. The bacterial mCherry signal was measured on day 0 and day 5 post infection on an Envision plate reader (PerkinElmer). Oleate was maintained throughout the experiment in the rescue assay conditions.

Measurement of total cellular ROS

Uninfected or *Mtb* infected macrophages monolayers in Ibidi eight-well chambers were stained with the CellROX Deep Red dye (Invitrogen) as per manufacturer's staining protocol. Live stained cells were imaged on a Leica SP5 confocal microscope. Z-stacks were re-constructed in ImageJ from which mean fluorescence intensities (MFI) for individual cells were obtained.

Datasets The RNA-seq data from the Dual RNA-seq analysis of infected mouse macrophages, which includes both macrophage and Mtb reads are available in GEO: GSE270571.

Acknowledgements

We would like to thank Dr. Jen K. Grenier and Ann E. Tate from the Cornell BRC Transcriptional Regulation and Expression Facility for their help with the development of dual RNA-Seq protocols. This work was supported by grants from the National Institutes of Health (AI155319, AI162598, and OD032135), Bill and Melinda Gates Foundation and the Mueller Health Foundation to D.G.R. EJ was supported by T32AI007349

551 **References**
552
553 1. WHO (2023) Global tuberculosis report 2023. World Health Organisation, Geneva,
554 Switzerland.

555 2. S. B. Cohen *et al.*, Alveolar Macrophages Provide an early *Mycobacterium tuberculosis*
556 niche and initiate dissemination. *Cell Host Microbe* **24**, 439-446.e434 (2018).

557 3. A. J. Wolf *et al.*, *Mycobacterium tuberculosis* infects dendritic cells with high frequency
558 and impairs their function in vivo. *J Immunol* **179**, 2509-2519 (2007).

559 4. P. Peyron *et al.*, Foamy macrophages from tuberculous patients' granulomas constitute a
560 nutrient-rich reservoir for *M. tuberculosis* persistence. *PLoS Pathog* **4**, e1000204 (2008).

561 5. D. G. Russell, P. J. Cardona, M. J. Kim, S. Allain, F. Altare, Foamy macrophages and the
562 progression of the human tuberculosis granuloma. *Nat Immunol* **10**, 943-948 (2009).

563 6. V. Singh *et al.*, *Mycobacterium tuberculosis*-driven targeted recalibration of macrophage
564 lipid homeostasis promotes the foamy phenotype. *Cell Host Microbe* **12**, 669-681 (2012).

565 7. J. Daniel, H. Maamar, C. Deb, T. D. Sirakova, P. E. Kolattukudy, Mycobacterium tuberculosis
566 uses host triacylglycerol to accumulate lipid droplets and acquires a dormancy-like
567 phenotype in lipid-loaded macrophages. *PLoS Pathog* **7**, e1002093 (2011).

568 8. E. J. Muñoz-Elías, J. D. McKinney, Mycobacterium tuberculosis isocitrate lyases 1 and 2 are
569 jointly required for in vivo growth and virulence. *Nat Med* **11**, 638-644 (2005).

570 9. A. K. Pandey, C. M. Sassetti, Mycobacterial persistence requires the utilization of host
571 cholesterol. *Proc Natl Acad Sci U S A* **105**, 4376-4380 (2008).

572 10. A. Brzostek, J. Pawelczyk, A. Rumijowska-Galewicz, B. Dziadek, J. Dziadek, Mycobacterium
573 tuberculosis is able to accumulate and utilize cholesterol. *J Bacteriol* **191**, 6584-6591
574 (2009).

11. L. Huang, E. V. Nazarova, S. Tan, Y. Liu, D. G. Russell, Growth of Mycobacterium tuberculosis in vivo segregates with host macrophage metabolism and ontogeny. *J Exp Med* **215**, 1135-1152 (2018).

12. D. Pisu, L. Huang, J. K. Grenier, D. G. Russell, Dual RNA-Seq of Mtb-Infected Macrophages In Vivo Reveals Ontologically Distinct Host-Pathogen Interactions. *Cell Rep* **30**, 335-350 e334 (2020).

13. D. Pisu *et al.*, Single cell analysis of M. tuberculosis phenotype and macrophage lineages in the infected lung. *J Exp Med* **218** (2021).

14. B. M. Cumming, K. W. Addicott, J. H. Adamson, A. J. Steyn, Mycobacterium tuberculosis induces decelerated bioenergetic metabolism in human macrophages. *Elife* **7** (2018).

15. M. Podinovskaia, W. Lee, S. Caldwell, D. G. Russell, Infection of macrophages with Mycobacterium tuberculosis induces global modifications to phagosomal function. *Cell Microbiol* **15**, 843-859 (2013).

16. M. J. Kim *et al.*, Caseation of human tuberculosis granulomas correlates with elevated host lipid metabolism. *EMBO Mol Med* **2**, 258-274 (2010).

17. Y. S. Kim *et al.*, PPAR-α Activation Mediates Innate Host Defense through Induction of TFEB and Lipid Catabolism. *J Immunol* **198**, 3283-3295 (2017).

18. P. E. Almeida *et al.*, Mycobacterium bovis bacillus Calmette-Guérin infection induces TLR2-dependent peroxisome proliferator-activated receptor gamma expression and activation: functions in inflammation, lipid metabolism, and pathogenesis. *J Immunol* **183**, 1337-1345 (2009).

19. M. Ouimet *et al.*, Mycobacterium tuberculosis induces the miR-33 locus to reprogram autophagy and host lipid metabolism. *Nat Immunol* **17**, 677-686 (2016).

598 20. S. P. Parihar *et al.*, Statin therapy reduces the mycobacterium tuberculosis burden in
599 human macrophages and in mice by enhancing autophagy and phagosome maturation. *J*
600 *Infect Dis* **209**, 754-763 (2014).

601 21. A. Singhal *et al.*, Metformin as adjunct antituberculosis therapy. *Sci Transl Med* **6**,
602 263ra159 (2014).

603 22. K. M. Wilburn, R. A. Fieweger, B. C. VanderVen, Cholesterol and fatty acids grease the
604 wheels of Mycobacterium tuberculosis pathogenesis. *Pathog Dis* **76** (2018).

605 23. M. Knight, J. Braverman, K. Asfaha, K. Gronert, S. Stanley, Lipid droplet formation in
606 Mycobacterium tuberculosis infected macrophages requires IFN-γ/HIF-1α signaling and
607 supports host defense. *PLoS Pathog* **14**, e1006874 (2018).

608 24. M. Bosch *et al.*, Mammalian lipid droplets are innate immune hubs integrating cell
609 metabolism and host defense. *Science* **370** (2020).

610 25. P. Chandra *et al.*, Inhibition of fatty acid oxidation promotes pacrophage control of
611 *Mycobacterium tuberculosis*. *mBio* **11**, e01139-20 (2020).

612 26. M. C. Kiritsy *et al.*, Mitochondrial respiration contributes to the interferon gamma
613 response in antigen-presenting cells. *Elife* **10**, e65109 (2021).

614 27. M. Hawkes *et al.*, CD36 deficiency attenuates experimental *Mycobacterial* infection. *BMC*
615 *Infect Dis* **10**, 299 (2010).

616 28. K. Nishiyama *et al.*, Fatty acid transport protein 1 enhances the macrophage inflammatory
617 response by coupling with ceramide and c-Jun N-terminal kinase signaling. *Intl*
618 *Immunopharmacol* **55**, 205-215 (2018).

619 29. A. Paul, B. H. Chang, L. Li, V. K. Yechoor, L. Chan, Deficiency of adipose differentiation-
620 related protein impairs foam cell formation and protects against atherosclerosis. *Circ Res*
621 **102**, 1492-1501 (2008).

30. G. Larigauderie *et al.*, Adipophilin enhances lipid accumulation and prevents lipid efflux from THP-1 macrophages: potential role in atherogenesis. *Arterioscler Thromb Vasc Biol* **24**, 504-510 (2004).

31. D. Conant *et al.*, Inference of CRISPR Edits from Sanger trace data. *CRISPR J* **5**, 123-130 (2022).

32. L. L. Listenberger, D. A. Brown, Fluorescent detection of lipid droplets and associated proteins. *Curr Protoc Cell Biol* **Chapter 24**, Unit 24.22 (2007).

33. A. R. Johnson *et al.*, Metabolic reprogramming through fatty acid transport protein 1 (FATP1) regulates macrophage inflammatory potential and adipose inflammation. *Mol Metab* **5**, 506-526 (2016).

34. L. E. Gleeson *et al.*, Cutting edge: *Mycobacterium tuberculosis* induces aerobic glycolysis in human alveolar macrophages that is required for control of intracellular bacillary replication. *J Immunol* **196**, 2444-2449 (2016).

35. L. Shi *et al.*, Infection with *Mycobacterium tuberculosis* induces the Warburg effect in mouse lungs. *Sci Rep* **5**, 18176 (2015).

36. M. Belton *et al.*, Hypoxia and tissue destruction in pulmonary TB. *Thorax* **71**, 1145-1153 (2016).

37. R. Courtnay *et al.*, Cancer metabolism and the Warburg effect: the role of HIF-1 and PI3K. *Mol Biol Rep* **42**, 841-851 (2015).

38. C. Li, J. Wang, J. F. Xu, J. Pi, B. Zheng, Roles of HIF-1α signaling in *Mycobacterium tuberculosis* infection: new targets for anti-TB therapeutics? *Biochem Biophys Res Commun* **711**, 149920 (2024).

39. D. Garcia, R. J. Shaw, AMPK: mechanisms of cellular energy sensing and restoration of metabolic balance. *Mol Cell* **66**, 789-800 (2017).

40. M. G. Gutierrez *et al.*, Autophagy is a defense mechanism inhibiting BCG and *Mycobacterium tuberculosis* survival in infected macrophages. *Cell* **119**, 753-766 (2004).

41. T. A. Gould, H. van de Langemheen, E. J. Muñoz-Elías, J. D. McKinney, J. C. Sacchettini, Dual role of isocitrate lyase 1 in the glyoxylate and methylcitrate cycles in *Mycobacterium tuberculosis. Mol Microbiol* **61**, 940-947 (2006).

42. J. D. McKinney *et al.*, Persistence of *Mycobacterium tuberculosis* in macrophages and mice requires the glyoxylate shunt enzyme isocitrate lyase. *Nature* **406**, 735-738 (2000).

43. E. J. Muñoz-Elías, A. M. Upton, J. Cherian, J. D. McKinney, Role of the methylcitrate cycle in *Mycobacterium tuberculosis* metabolism, intracellular growth, and virulence. *Mol Microbiol* **60**, 1109-1122 (2006).

44. J. E. Griffin *et al.*, Cholesterol catabolism by *Mycobacterium tuberculosis* requires transcriptional and metabolic adaptations. *Chem Biol* **19**, 218-227 (2012).

45. S. Savvi *et al.*, Functional characterization of a vitamin B12-dependent methylmalonyl pathway in *Mycobacterium tuberculosis*: implications for propionate metabolism during growth on fatty acids. *J Bacteriol* **190**, 3886-3895 (2008).

46. W. Lee, B. C. VanderVen, R. J. Fahey, D. G. Russell, Intracellular Mycobacterium tuberculosis exploits host-derived fatty acids to limit metabolic stress. *J Biol Chem* **288**, 6788-6800 (2013).

47. N. V. Simwela *et al.*, Genome-wide screen of *Mycobacterium tuberculosis* infected macrophages identified the GID/CTLH complex as a determinant of intracellular bacterial growth. *bioRxiv* 10.1101/2024.05.06.592714, 2024.2005.2006.592714 (2024).

48. T. Wu *et al.*, clusterProfiler 4.0: a universal enrichment tool for interpreting omics data. *Innovation (Camb)* **2**, 100141 (2021).

49. A. Vogel, J. S. Brunner, A. Hajto, O. Sharif, G. Schabbauer, lipid scavenging macrophages and inflammation. *Biochim Biophys Acta Mol Cell Biol Lipids* **1867**, 159066 (2022).

671 50. R. J. Raggers, A. van Helvoort, R. Evers, G. van Meer, The human multidrug resistance
672 protein MRP1 translocates sphingolipid analogs across the plasma membrane. *J Cell Sci*
673 **112 (Pt 3)**, 415-422 (1999).

674 51. E. Campos-Pardos, S. Uranga, A. Picó, A. B. Gómez, J. Gonzalo-Asensio, Dependency on
675 host vitamin B12 has shaped *Mycobacterium tuberculosis* complex evolution. *Nat*
676 *Commun* **15**, 2161 (2024).

677 52. B. Bazet Lyonnet *et al.*, Pleiotropic effect of AccD5 and AccE5 depletion in acyl-coenzyme
678 A carboxylase activity and in lipid biosynthesis in *Mycobacteria*. *PLoS One* **9**, e99853
679 (2014).

680 53. N. A. Lack *et al.*, Characterization of a carbon-carbon hydrolase from *Mycobacterium*
681 *tuberculosis* involved in cholesterol metabolism. *J Biol Chem* **285**, 434-443 (2010).

682 54. D. Schnappinger *et al.*, Transcriptional adaptation of *Mycobacterium tuberculosis* within
683 macrophages: insights into the phagosomal environment. *J Exp Med* **198**, 693-704 (2003).

684 55. D. F. Warner, J. C. Evans, V. Mizrahi, Nucleotide Metabolism and DNA Replication.
685 *Microbiol Spectr* **2**, MGM2-0001-2013 (2014).

686 56. J. S. Lott, The tryptophan biosynthetic pathway is essential for *Mycobacterium*
687 *tuberculosis* to cause disease. *Biochem Soc Trans* **48**, 2029-2037 (2020).

688 57. M. E. Theriault *et al.*, Iron limitation in *M. tuberculosis* has broad impact on central carbon
689 metabolism. *Commun Biol* **5**, 685 (2022).

690 58. T. C. Zahrt, J. Song, J. Siple, V. Deretic, Mycobacterial FurA is a negative regulator of
691 catalase-peroxidase gene KatG. *Mol Microbiol* **39**, 1174-1185 (2001).

692 59. J. S. Kim, Y. R. Kim, C. S. Yang, Host-directed therapy in tuberculosis: targeting host
693 metabolism. *Front Immunol* **11**, 1790 (2020).

60. M. D. Fullerton *et al.*, Single phosphorylation sites in Acc1 and Acc2 regulate lipid homeostasis and the insulin-sensitizing effects of metformin. *Nat Med* **19**, 1649-1654 (2013).

61. T. Matsufuji *et al.*, Arylpiperazines as fatty acid transport protein 1 (FATP1) inhibitors with improved potency and pharmacokinetic properties. *Bioorg Med Chem Lett* **23**, 2560-2565 (2013).

62. L. Deng, S. Kersten, R. Stienstra, Triacylglycerol uptake and handling by macrophages: from fatty acids to lipoproteins. *Progress in Lipid Research* **92**, 101250 (2023).

Figure legends

Fig.1 Knockdown of fatty acid import and metabolism genes restricts *Mtb* growth in macrophages. (A) Schematic of lipid import and metabolism genes in macrophages. Genes targeted for CRISPR-Cas9 mediated knockdown are highlighted in red. (B-C) Scramble or indicated mutant macrophages were infected with the *Mtb* Erdman strain at MOI 0.4. CFUs were plated 3 hours post infection (B) and on Day 5 (C) to determine intracellular *Mtb* replication rates. n=6; ****, $P < 0.0001$.

Fig. 2. *Mtb* infected macrophages with impaired fatty acid import and metabolism display reduced mitochondrial activities and are more glycolytic. (A) Seahorse flux analyses of scramble or PLIN2$^{-/-}$, FATP1$^{-/-}$ and CPT2$^{-/-}$ macrophages infected with *Mtb* Erdman strain at MOI 1 24 hours post infection. Oxygen consumption rates (OCR) were measured using the Cell Mito Stress Test Kit (Agilent). Oligo, oligomycin; FCCP, fluoro-carbonyl cyanide phenylhydrazone; Rot/A, rotenone and antimycin A. (B) Comparison of basal respiration and spare respiratory capacity (SRC) from A. SRC was calculated by subtracting the normalized maximal OCR from basal OCR. n=3 (2 technical repeats per replicate); ****, $P < 0.0001$. (C) Extracellular acidification rates (ECARs) of scramble or PLIN2$^{-/-}$, FATP1$^{-/-}$ and CPT2$^{-/-}$ macrophages infected with *Mtb* as in A. ECARs were measured using the Agilent Seahorse Glycolysis Stress Test kit. 2DG, 2-Deoxy-D-glucose. (D) Comparison of basal glycolysis and spare glycolytic capacity (SGC) in the indicated mutant macrophages. SGC was calculated as SRC above. n=3 (2 technical repeats per replicate); *, $P < 0.05$, ****, $P < 0.0001$.

Fig. 3. Knockdown of fatty acid import and metabolism genes in macrophagesactivate AMPK and stabilizes HIF-1α. (A) Western blot analysis of HIF-1α in uninfected and *Mtb* infected scramble or PLIN2$^{-/-}$, FATP1$^{-/-}$ and CPT2$^{-/-}$ macrophages. In *Mtb* infected conditions, cells were infected with the bacteria at MOI 1 for 48 hours before preparation of cell lysates. (B) Western blot analysis of total and phosphorylated AMPK in uninfected and *Mtb* infected scramble or PLIN2$^{-/-}$, FATP1$^{-/-}$ and CPT2$^{-/-}$ *macrophages*. Cell lysates were prepared as in A.

Fig. 4. Supplementation with exogenous oleate fails to rescue the *Mtb* Δicl1 mutant in PLIN2$^{-/-}$, FATP1$^{-/-}$ and CPT2$^{-/-}$ macrophages. (A) Scramble or indicated mutant macrophages were infected with the *Mtb* H37Rv Δicl1 mutant expressing mCherry at MOI 5. Oleate supplementation (400 μM) was commenced 24 hours before infection in the treatment group, removed during *Mtb* infection and re-added 3-hours post infection for the entire duration of the experiment. Growth kinetics of *Mtb* were measured by monitoring mCherry fluorescence using a plate reader. n=4; ****, $P < 0.0001$. (B) Uninfected scramble or FATP1$^{-/-}$ and CPT2$^{-/-}$ macrophages were supplemented with 400 μM oleate for 24 hours. Cells were then fixed for 20 minutes and stained for lipid droplet inclusions using the Bodipy 493/503 dye. DAPI was used as a counterstain to detect nuclei.

Fig. 5. Dual RNA sequencing to identify host and bacterial determinants of *Mtb* restriction in macrophages with fatty acid import and metabolism knockdown genes. (A) Principal component analysis (PCA) of scramble or PLIN2$^{-/-}$, FATP1$^{-/-}$ and CPT2$^{-/-}$ macrophages transcriptomes infected with the *Mtb* smyc'::mCherry strain at MOI 0.5 4 days post infection. (B) Venn diagram of DE gene sets (Table S2) in PLIN2$^{-/-}$, FATP1$^{-/-}$ and CPT2$^{-/-}$ mutant macrophages as compared to scramble showing overlapping genes. DE genes cutoff; abs (log_2 fold change) > 0.3, adjusted p-value < 0.05. (C-D) Tree plot of top 80 enriched gene ontology terms (biological process) in *Mtb* infected PLIN2$^{-/-}$ and FATP1$^{-/-}$ upregulated genes.

Fig. 6. Nutritional and oxidative stress define the core transcriptome response of *Mtb* inside PLIN2$^{-/-}$ macrophages. (A) Schematic showing DE genes in *Mtb* transcriptomes isolated from PLIN2$^{-/-}$, FATP1$^{-/-}$ and CPT2$^{-/-}$ macrophages in Fig.5A. (B) Heatmaps of nutritional and oxidative stress DE genes in PLIN2$^{-/-}$ macrophages. Arrows show genes which are also DE in CPT2$^{-/-}$ macrophages in a similar trend (Table S4).

Fig. 7. Inhibitors of fatty acid transport and metabolism block intracellular growth of *Mtb* in macrophages. (A) Growth of *Mtb* in liquid broth in the absence of drug (DMSO) or presence of metformin, FATP1 inhibitor (FATP1 In, 10 μM) and the β-oxidation of fatty acid inhibitor,

Trimetazidine (TMZ, 500 nM). *Mtb* Erdman was grown to log phase and diluted to OD_{600} 0.01 in 7H9 media in the presence of the above inhibitors. Growth kinetics were monitored by OD_{600} measurements using a plate reader. Rifampicin (RIF) at 0.5 μg/ml was used as a total killing control. (B) Scramble macrophages were infected with *Mtb* Erdman at MOI 0.5. Inhibitors were added 3 hours post infection following which CFUs were plated 4 days post infection. n=5; **, $P < 0.01$; ****, $P < 0.0001$.

808 **Figure 1.**

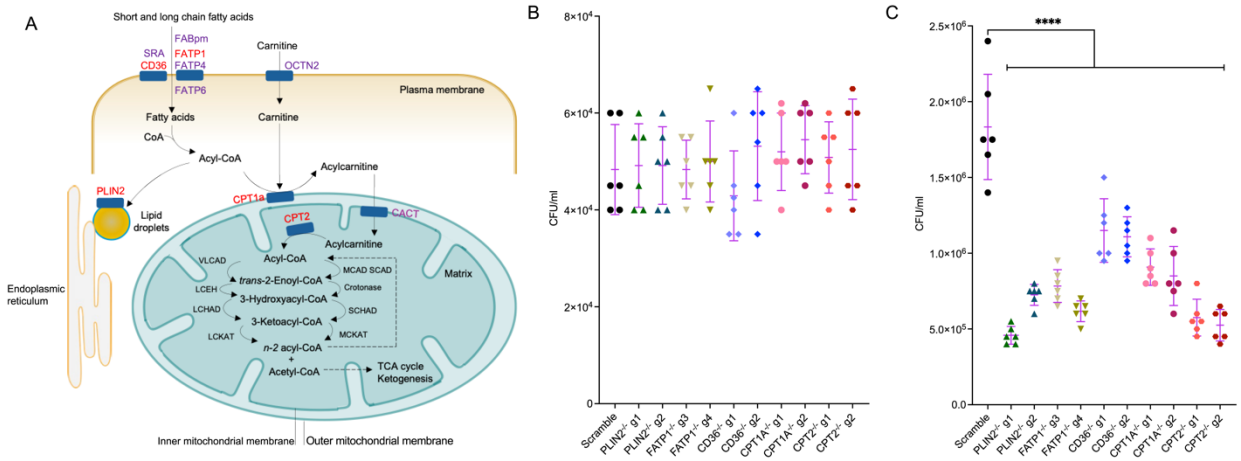

809

810

811 **Figure 2**

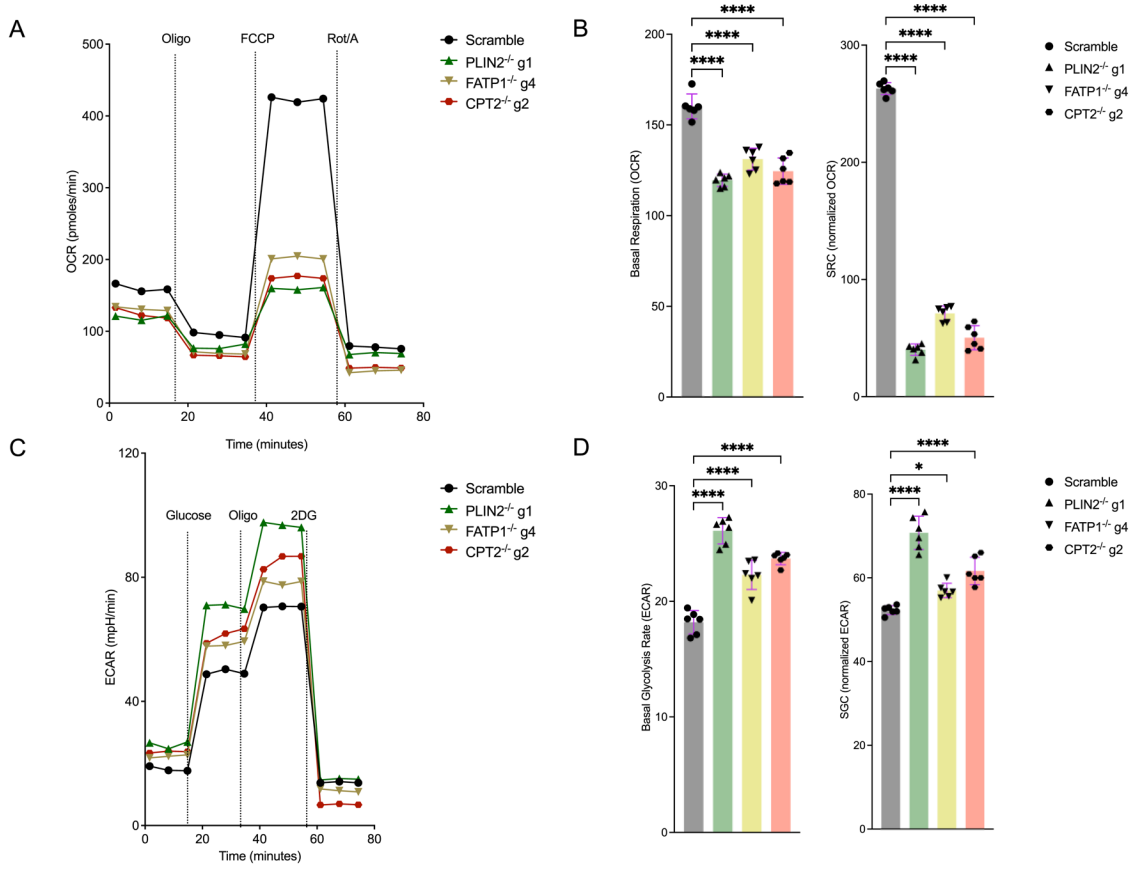

812

813

814 **Figure 3**

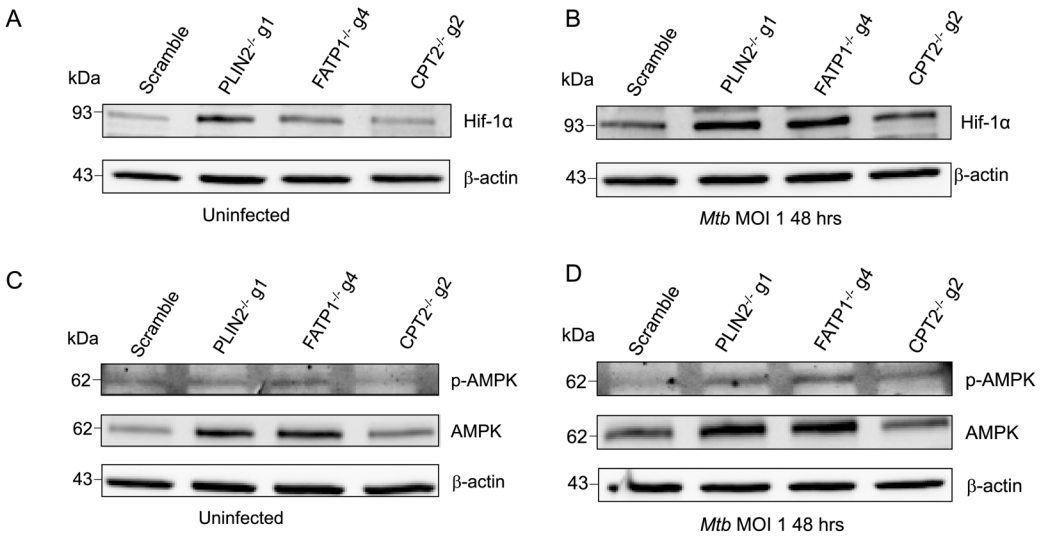

815

816

817 **Figure 4.**

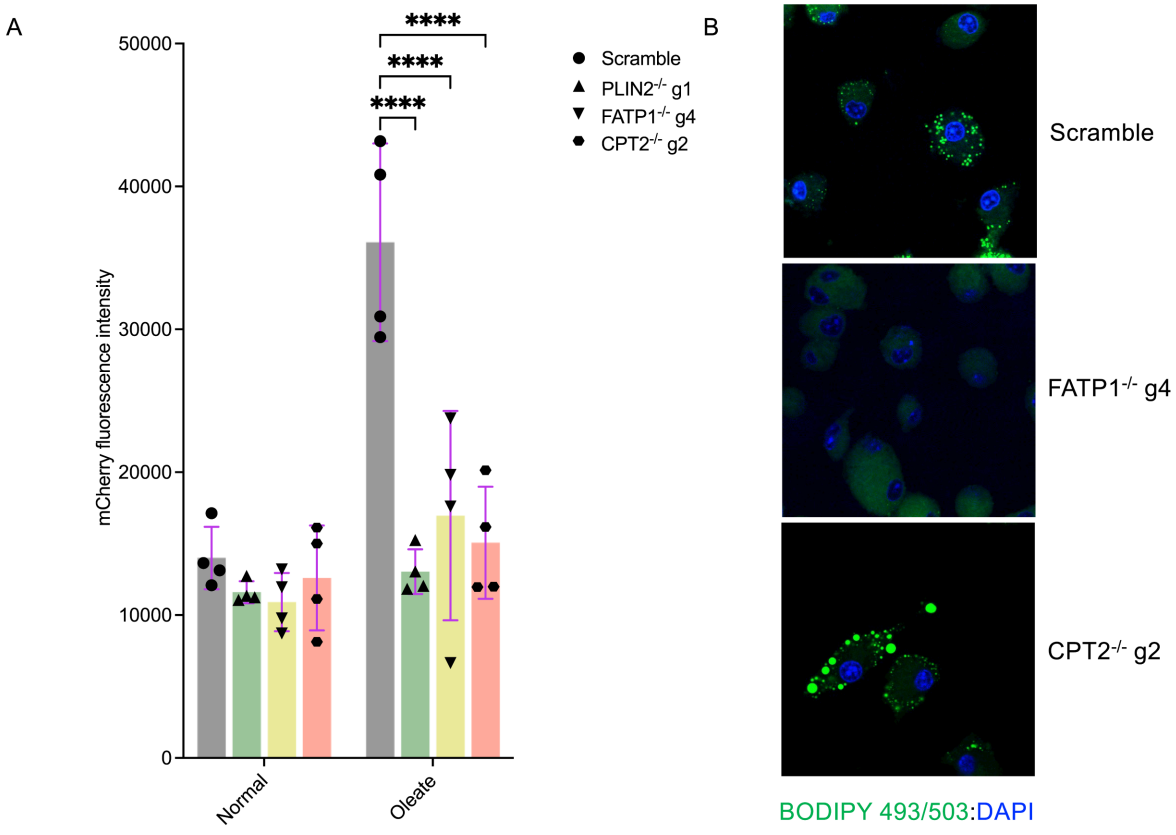

818

819

820 **Figure 5.**

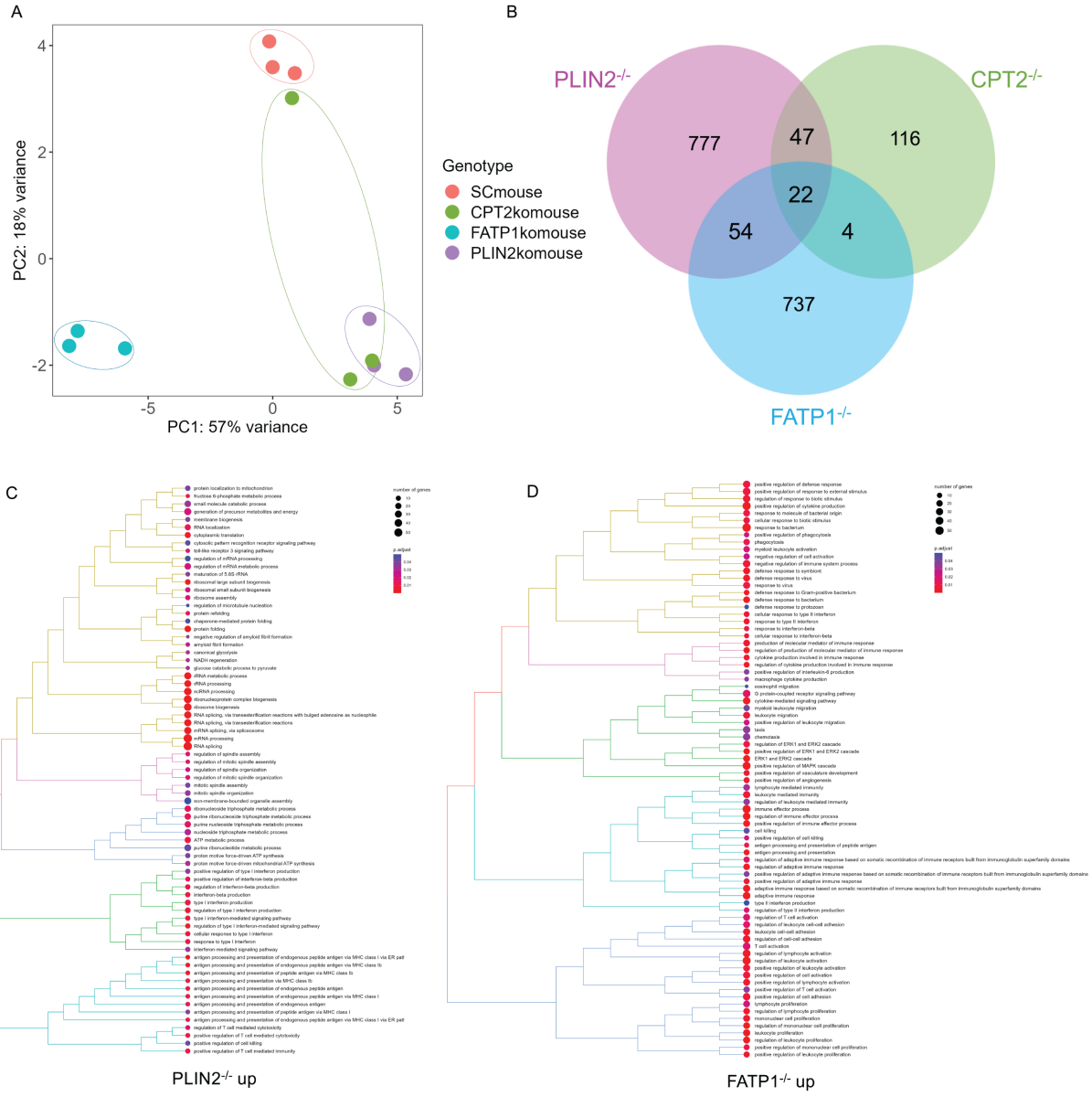

821

822

823

824 **Figure 6.**

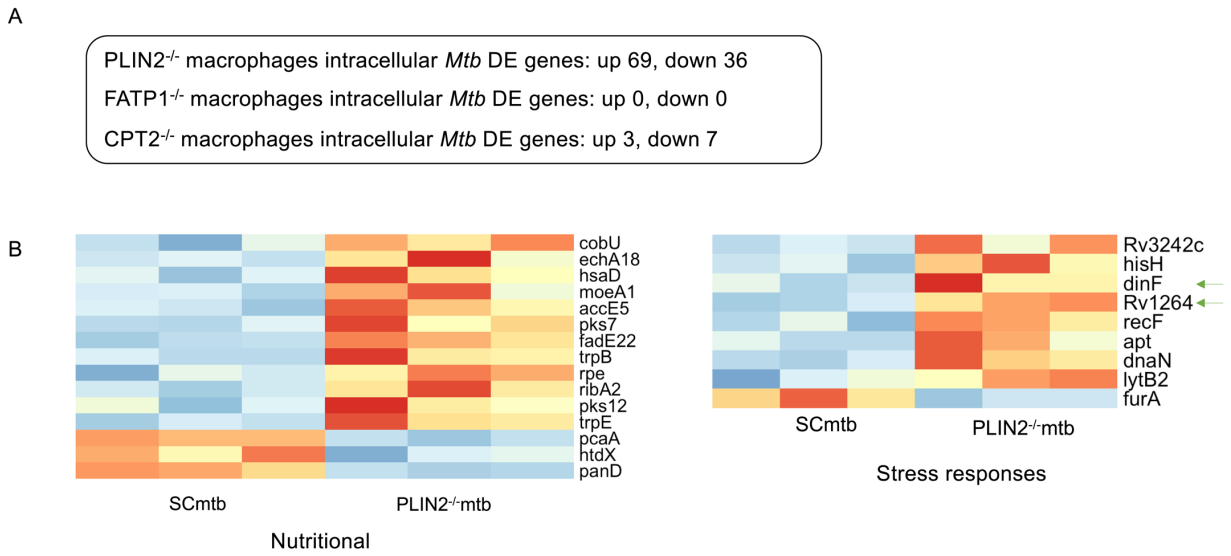

825

826 **Figure 7.**

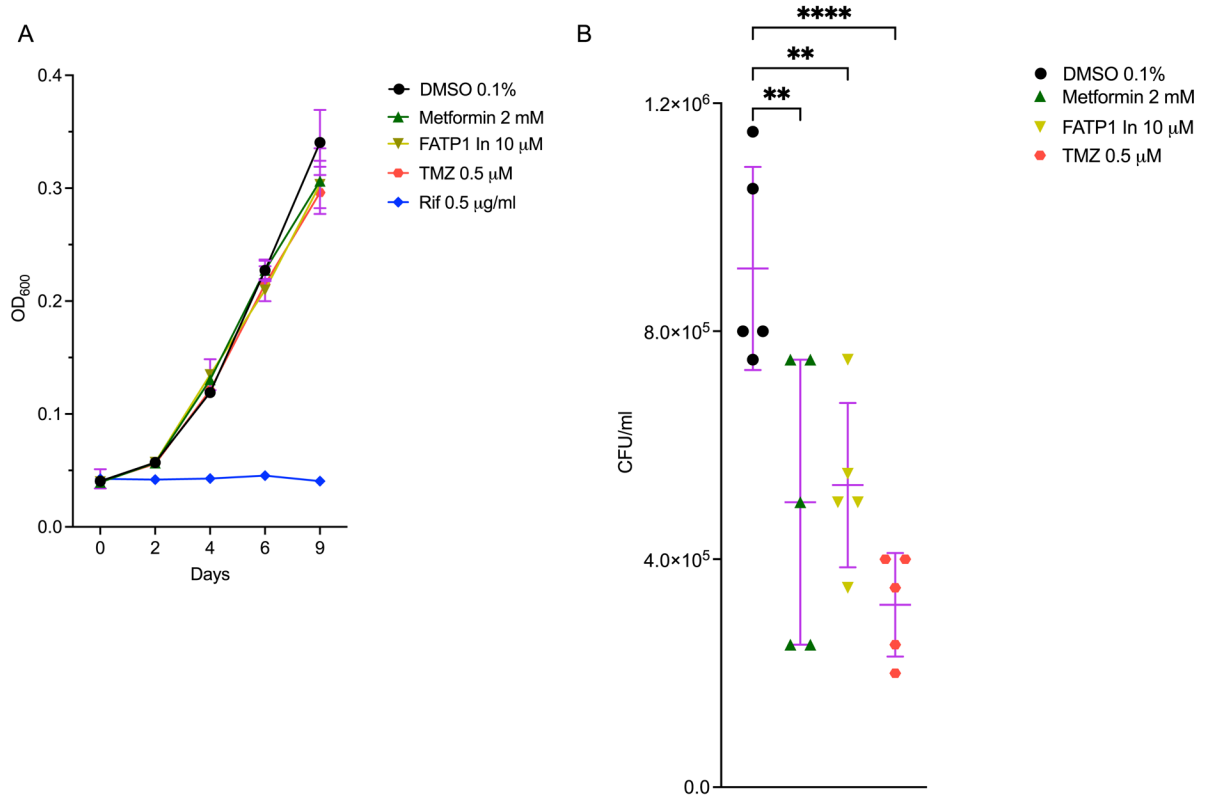

827

828